Electrochimica Acta, 1972, Vol. 17, pp. 1723 to 1734. Pergamon Press. Printed in Northern Ireland

KINETICS OF THE $SCN^-/(SCN)_2$ COUPLE ON PLATINUM IN ACETONITRILE*

R. PEREIRO, A. J. ARVÍA and A. J. CALANDRA
Instituto de Investigaciones Fisicoquímicas Teóricas y Aplicadas, División Electroquímica, Facultad de Ciencias Exactas, Universidad Nacional de La Plata, La Plata, Argentina

Abstract—The electrode kinetics of the $SCN^-/(SCN)_2$ system has been studied on platinum in the temperature range from −12 to −3°C at different ammonium thiocyanate concentrations in acetonitrile in the presence of 0·1 M $[(C_2H_5)_4N]ClO_4$. Quasi-steady *E/I* curves with a Pt rotating disk electrode and *E/I* curves at different linear potential-sweep rates were recorded under different experimental conditions.

Both reactions of the pseudohalogen electrode are rather slow processes, the kinetics of which can be explained with the same mechanistic formalism postulated for the halogen electrodes in acetonitrile.

Résumé—Etude de la cinétique électrochimique du système $SCN^-/(SCN)_2$, sur électrode de platine, dans un domaine de températures de −12 à −3°C, pour différentes concentrations en thiocyanate d'ammonium dans l'acétonitrile, en présence de $[(C_2H_5)_4N]ClO_4$ 0,1 M. Courbes quasi-stationnaires E/I sur électrode à disque de platine tournant et courbes E/I à différentes vitesses linéaires de balayage de potentiel, dans des conditions expérimentales variées.

Les deux réactions de l'électrode à pseudo-halogène correspondent à des processus plutôt lents, leurs cinétiques peuvent s'expliquer selon le mécanisme précédemment postulé pour les électrodes à halogène dans l'acétonitrile.

Zusammenfassung—Es wurde die Elektroden-Kinetik des $SCN^-/(SCN)_2$-Systems an Platinelektroden im Temperaturbereich von −12 bis −3°C unter Anwendung verschiedener Thiocyanatkonzentrationen in Acetonitril in Gegenwart von 0,1 M $[(C_2H_5)_4N]ClO_4$ untersucht. Unter verschiedenen experimentellen Bedingungen wurden quasistationäre *E/I*-Kurven an einer rotierenden Platinscheibenelektrode und *E/I*-Kurven bei verschiedenen linearen Potentialschwenkgeschwindigkeiten aufgenommen.

Beide Reaktionen der Pseudo-Halogenelektrode sind ziemlich langsame Prozesse, deren Kinetik mit dem gleichen Mechanismus erklärt werden kann, wie er für die Halogen-Elektroden in Acetonitril formuliert wurde.

INTRODUCTION

SEVERAL decades ago, the electrochemical oxidation of SCN^- ion in methanol solution on platinum and silver electrodes was studied[1] and the reaction product was identified as thiocyanogen, $(SCN)_2$. The anodic oxidation of SCN^- ion in aqueous media yielded as final products SO_4^{2-} and H^+ ions, probably after the occurrence of a chemical reaction between the product of the electrode process and the solvent.[2–5] The electrolysis of alkali thiocyanates in mixtures of organic solvent and water has been used for thiocyanation of aromatic compounds.[6,7]

A recent publication on the electrochemical properties of the SCN^- ion and $(SCN)_2$ in acetonitrile[8] reveals that a relatively slow electrode process is involved in the oxidation of SCN^- ion in acetonitrile solutions at −10°C and the corresponding half-wave potential is rather poorly reproducible. The voltamperometric curves are in agreement with the hypothesis of a rapid dimerization of the SCN radical, which is the primary product of the anodic initial electron-transfer step. A cathodic limiting current related to the electrochemical reduction of $(SCN)_2$ has been also measured.[8]

The reaction involving the initial discharge of the SCN^- ion on platinum at temperatures above room temperature, yielding as final product parathiocyanogen as

* Manuscript received 30 September 1971.

an insoluble film on the electrode, has been studied both in acetonitrile and dimethylsulphoxide,[9–10] as well as in molten potassium thiocyanate[11,12]. The kinetics of this electrode process was thoroughly investigated because of its significance for the theory of electrochemical film formation. The total process involves a polymerization reaction which definitely occurs after the initial electrochemical oxidation of the SCN^- ion. Therefore, for a quantitative investigation of this reaction with a minimum interference of polymer formation, experiments have to be performed at the lowest possible temperature. For the purpose, acetonitrile was chosen as an adequate solvent, because of its low freezing point.

The fact that the SCN^- ion is isoelectronic with the halide ions as the SCN radical and $(SCN)_2$ molecule are to the halogen atoms and halogen molecules respectively suggests that the electrochemical behaviour of the $SCN^-/(SCN)_2$ couple may be like that of the halogen electrodes which, except for fluorine, have been recently investigated from the kinetic and mechanistic viewpoint, on platinum electrodes in acetonitrile.[13–15] The conclusions of these studies indicate the occurrence of a common formal mechanism related to the halogen electrodes in acetonitrile and it seems quite reasonable that if the $SCN^-/(SCN)_2$ couple can be properly isolated and its kinetic parameters evaluated, the same formal reaction mechanism would apply to the pseudo-halogen electrode.

EXPERIMENTAL TECHNIQUE

A three-compartment electrolysis cell similar to that described in previous work[16] was employed. A platinum rotating disk working electrode and a platinum counter-electrode were used. An arbitrary platinum wire electrode, of which the potential was reproducible and stable, was used as reference.

Solutions of ammonium thiocyanate (Merck, AR) and tetra-ethylammonium perchlorate (Eastman Chemicals) in acetonitrile (U.C.B., AR) were employed. The solid $(NH_4)SCN$ was dried at 60–70°C under vacuum and the solid $[(C_2H_5)_4N]ClO_4$ was also vacuum-dried at room temperature. The solvent was purified following a procedure indicated in the literature[17] and stored under a dry and inert atmosphere. The $(NH_4)SCN$ concentration was varied from $0{\cdot}8 \times 10^{-3}$ to 2×10^{-3} M. The concentration of $[(C_2H_5)_4N]ClO_4$, which acted as supporting electrolyte, was 0·1 M.

Experiments were performed in the temperature range from −12 to −3°C, by using the rotating disk electrode technique to obtain stationary current/potential curves and linear potential-sweep cyclic voltammetry, to record non-stationary current/potential curves. The former technique was applied with a potential sweep of 2 mV/s, which yielded the same E/I response as those at lower rates, and rotation speeds of the working electrode covering from 150 to 2600 rev/min. The latter was applied at potential-sweep rates from 5 to 350 mV/s, covering a potential amplitude of $0{\cdot}580 \pm 0{\cdot}010$ V.

RESULTS

1. *Experiments with rotating disk electrodes*

The solution, which was initially colourless, acquired a yellow tinge in the anodic section of the electrolysis cell after being repeatedly used in the anodic runs.

Typical E/I curves obtained on the platinum rotating disk electrode are illustrated in Fig. 1. Initially at low anodic polarization, these curves show practically no current flow. On increasing the polarization about 0·2–0·3 V above the initial potential E_i, a net current increase is observed, reaching a plateau at about 1·0 V.

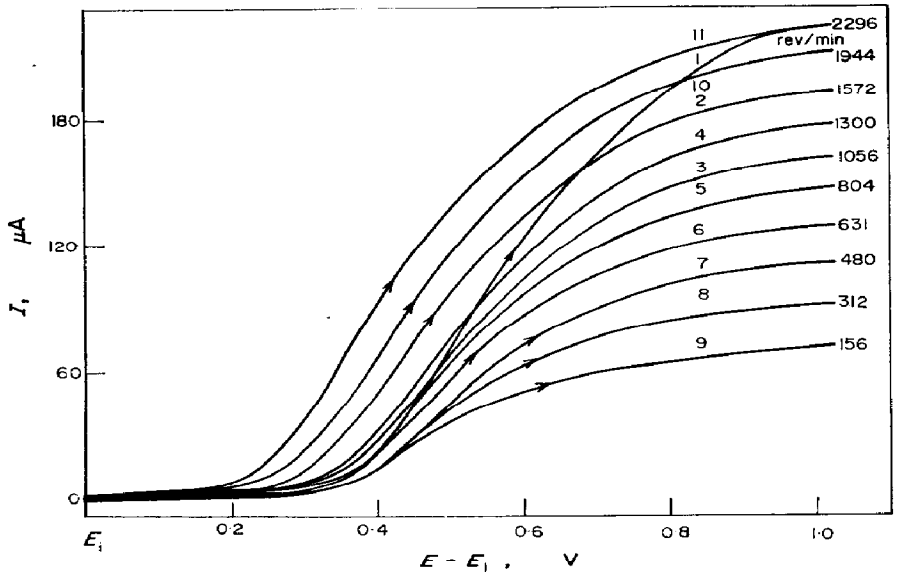

FIG. 1. Anodic current/potential curves obtained at $v = 2$ mV/s and different rotation speeds of the Pt working electrode as indicated in the figure. The numbers on the curves correspond to the sequence of the experiments.
c_0, $2{\cdot}016 \times 10^{-3}$ M; TEAP, 0·1 M; −5·0°C; A, 0·071 cm².

A distinction in the curves of the figure has to be made between the first run starting with a recently polished electrode surface and the subsequent runs. The former exhibits a larger polarization effect than the following ones and for a run under fixed experimental conditions, the returning E/I curve involves a net depolarizing effect (Fig. 2). In any circumstance, the limiting current region is attained

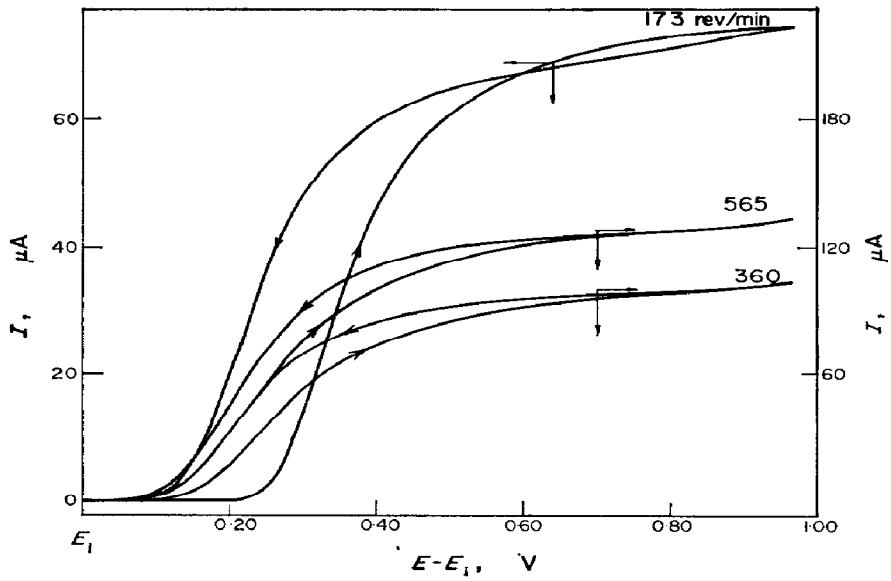

FIG. 2. Anodic current/potential curves obtained on a Pt rde at $v = +2$ mV/s and $v = -2$ mV/s and different rotation speeds.
$c_0 = 2{\cdot}028 \times 10^{-3}$ M; TEAP, 0·1 M; −1·0°C; A, 0·071 cm².

asymptotically and it extends no further than 0·1 V or thereabouts. These experiments show the different behaviour of freshly polished and repeatedly used electrodes and also show that reproducible electrode surface conditions must be achieved in order to derive useful kinetic data from the E/I curves.

In spite of this, some relationships corresponding to the electrode process under convective–diffusion control can be tested. Thus, experimental results show that the limiting current, I_L, depends linearly both on the square root of the rotation speed, ω, and on the concentration of dissolved thiocyanate, c_0 (Fig. 3).

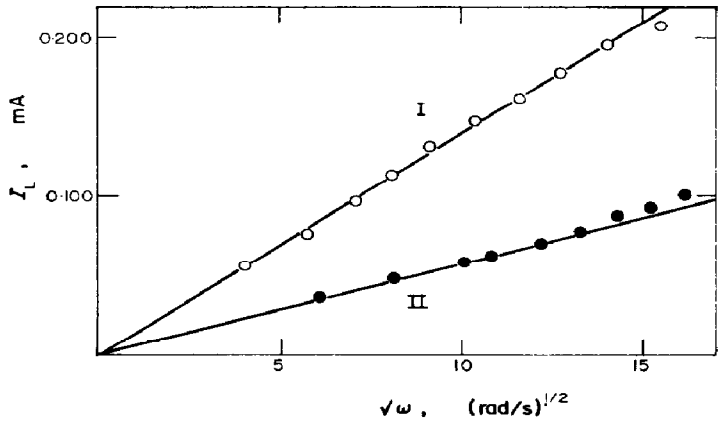

FIG. 3. Dependence of the anodic limiting current on the rotation speed of the working electrode.
I, $c_0 = 2{\cdot}016 \times 10^{-3}$ M; TEAP, 0·1 M; −5·0°C.
II, $c_0 = 0{\cdot}81 \times 10^{-3}$ M; TEAP, 0·1 M; −4·5°C.

In order to determine the shift of the electrode half-wave potential for the anodic reaction, $(E_{1/2})_a$, independent runs with reproducible electrode surfaces were made (Fig. 4). This indicates that $(E_{1/2})_a$ changes linearly with the logarithm of the

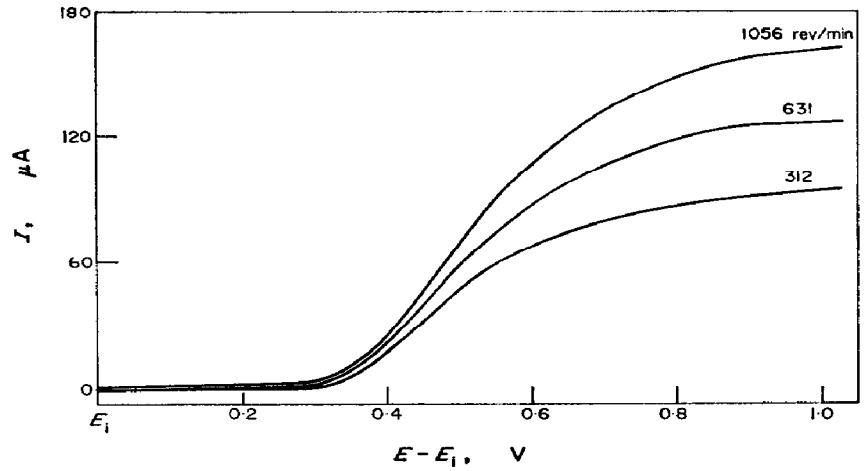

FIG. 4. Anodic current/potential curves obtained at three different rotation speeds with an aged Pt electrode.
c_0, $2{\cdot}016 \times 10^{-3}$ M; TEAP, 0·1 M; −1·0°C; A, 0·071 cm².

rotation speed, becoming more positive as ω increases. The slope of the straight line in the $(E_{1/2})_a$ *vs* log $\omega^{1/2}$ is practically $2{\cdot}3(2RT/F)$, as seen in Fig. 5.

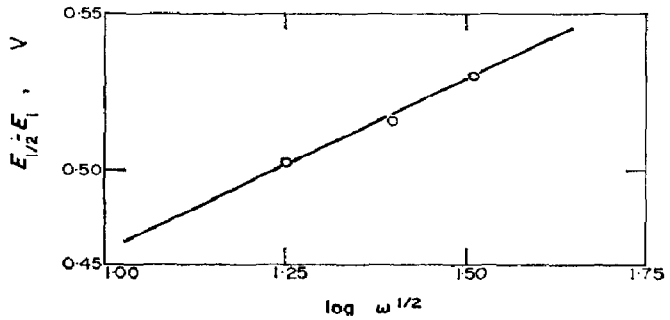

FIG. 5. Dependence of the anodic half-wave potential on the *E/I* curves shown in Fig. 4 on the rotation speed of the working electrode.

The *E/I* curves, at lower anodic potentials, above E_i, exhibit a negligible influence of the rotation speed on the current.

2. *Results obtained from triangular wave voltammetry*

Typical sets of voltammetric runs are seen in Figs. 6 and 7. They show an anodic current peak, I_{ap}, and a cathodic current peak, I_{cp}. The former is well defined for

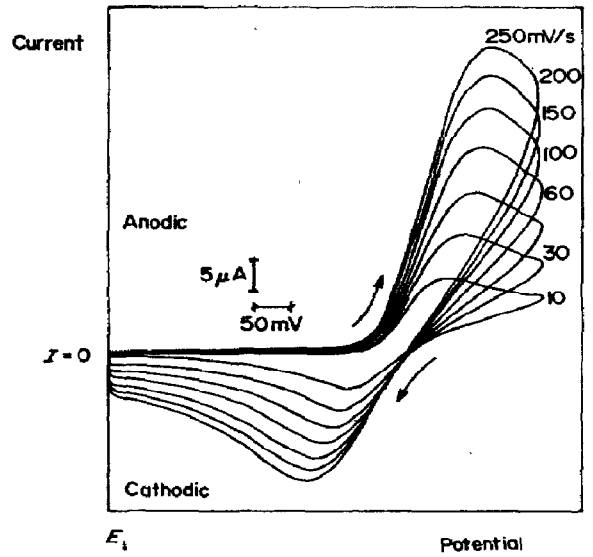

FIG. 6. *E/I* single sweep cyclic voltammetric curves on Pt at different sweep rates. c_o, $2{\cdot}028 \times 10^{-3}$ M; TEAP, 0·1 M; −10·0°C; *A*, 0·071 cm^2.

potential-sweep rates larger than 10 mV/s; at lower rates it appears as an anodic limiting current.

It is clearly established that the height of both peaks increases with the potential-sweep rate and with the concentration of dissolved thiocyanate in the solution. The potential at which the anodic current maximum occurs, E_{ap}, shifts toward more positive potentials when the potential-sweep rate, v, increases. The reverse effect

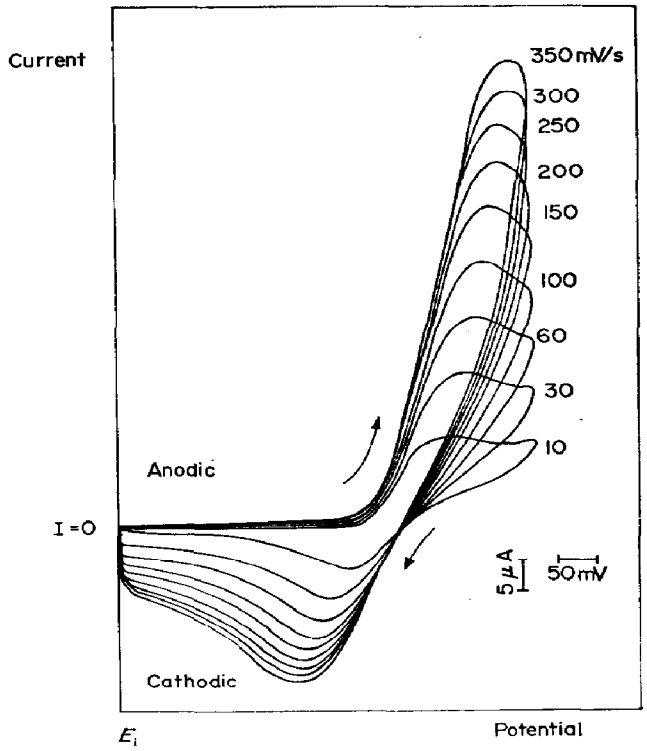

FIG. 7. E/I single sweep cyclic voltammetric curves on Pt at different sweep rates. c_0, $2{\cdot}028 \times 10^{-3}$ M; TEAP, 0·1 M; −3·0°C; A, 0·071 cm².

occurs on the potential associated with the cathodic current maximum, E_{cp}. The cathodic peak is better defined in the E/I voltagrams run at the lower temperature.

Various relationships are established for the kinetic parameters involved in the voltammetric E/I curves. The actual magnitude of the cathodic current peak obtained during the returning half-cycle was evaluated with the semi-empirical equation mentioned in the literature.[18]

Both the anodic and the cathodic current peaks approach a straight line intercepting the origin of co-ordinates when they are plotted as a function of the square root of the potential sweep rate, Fig. 8. The best straight line, however, exhibits at higher potential-sweep rates a slight curvature, probably due to an ohmic effect which, for this case, implies a constant factor of 0·9, so that the measured anodic current peak is 0·9 times the true anodic current peak.[19] This effect also exists in the cathodic current peak *vs* $v^{1/2}$ plot.

The ratio between true maximum anodic current peak to true maximum cathodic current peak is on the average 0·95 as indicated in Table 1.

The potentials associated with both the anodic and the cathodic current peak change linearly with the logarithm of v, as shown in Fig. 9. The slope of the straight line derived from the $(E_p - E_i)$ *vs* log v plot is $2{\cdot}3(RT/F)$ V/decade.

Finally, potentials related either to the anodic or the cathodic current peak also depend linearly on the logarithm of the corresponding current maximum (Fig. 10). Both $E/\log I_p$ plots exhibit a slope very close to $2{\cdot}3(2RT/F)$. In this case a trend to deviate from the straight line is observed for data corresponding to the higher sweep

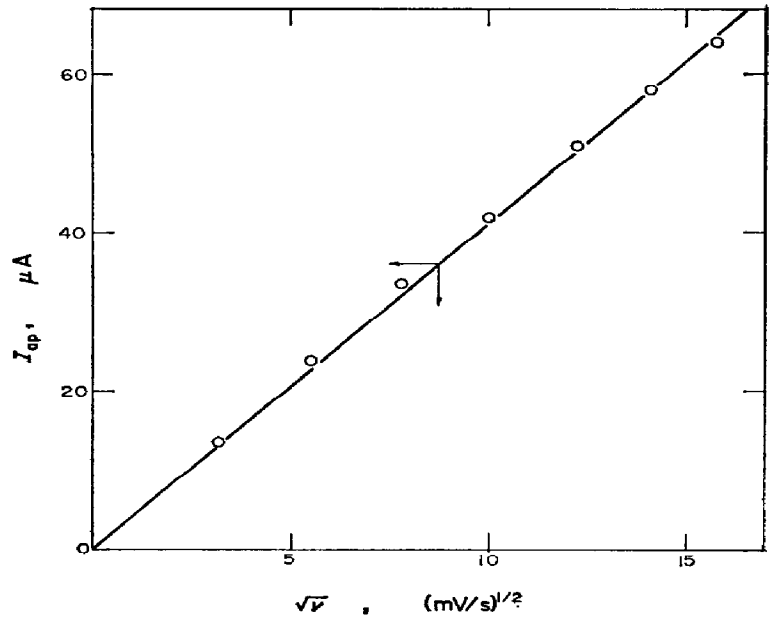

FIG. 8. Dependence of the anodic current peak on the potential sweep rate.
c_0, 2·028 × 10^{-3} M; TEAP, 0·1 M; −3·0°C.

TABLE 1. CURRENT MAXIMA CALCULATED FROM *E/I* VOLTAMMETRIC CURVES

v mV/s	I_{ap} μA	I_{ap}/I_{cp}	I_{cp} μA
10	11·5	0·967	11·1
30	18·3	0·953	17·4
60	25·0	0·953	23·8
100	32·0	0·939	30·1
150	38·5	0·943	36·3
200	43·5	0·953	41·5
250	48·5	0·946	45·9

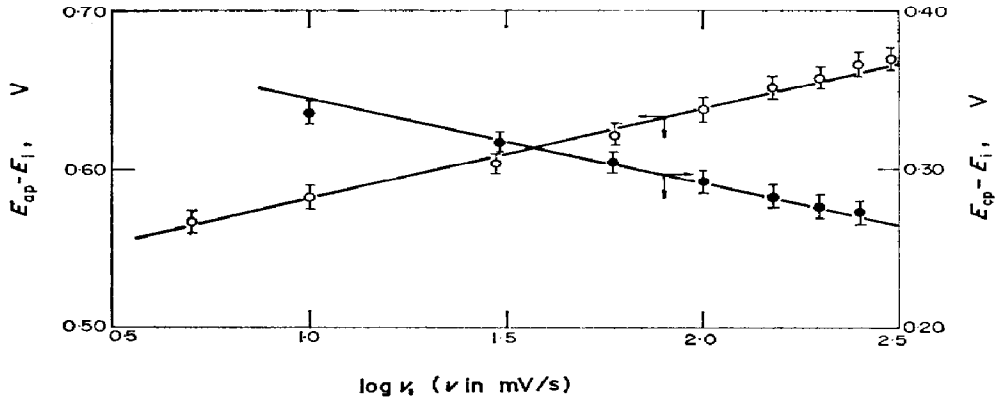

FIG. 9. Dependence of the potentials corresponding to the anodic and cathodic current maxima on the potential-sweep rate.
c_0, 0·085 × 10^{-3} M; TEAP, 0·1 M; −4°C.

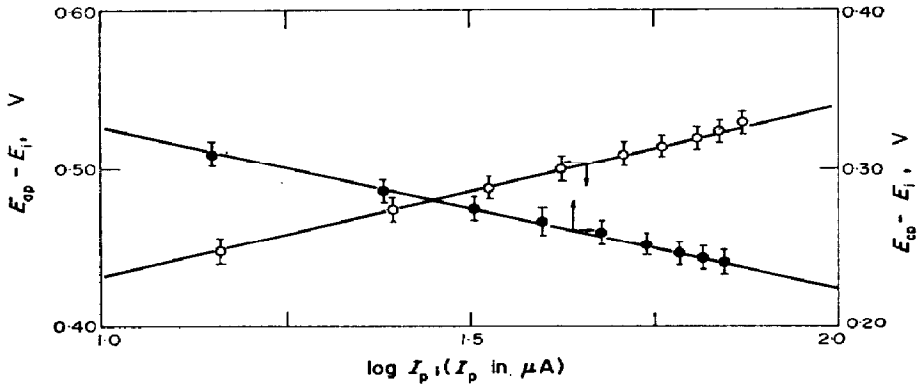

FIG. 10. Semilogarithmic plots of the potentials at the current maxima *vs* the corresponding current maxima.
c_0, $2{\cdot}028 \times 10^{-3}$ M; TEAP, 0·1 M; −3°C.

rates because of the existence of a pseudo-ohmic polarization which slightly distorts the voltammetric *E/I* curves, producing a decrease of the current maxima and a small additional potential shift. This difficulty can be overcome by measuring the pseudo-ohmic polarization independently.

INTERPRETATION AND DISCUSSION

The reaction occurring at the platinum anodes is the electrochemical oxidation of SCN^- ions yielding as final product thiocyanogen, and the latter can be reduced cathodically. Then the over-all reaction at the electrode is

$$2\,SCN^- \rightleftarrows (SCN)_2 + 2\,e. \qquad (1)$$

The chemical reactivity of $(SCN)_2$ is well known, but at low temperatures in the ACN medium it is stable enough[8] to be reduced during the returning potential sweep in cyclic voltammetry. The solvent itself may contribute to stabilize the dissolved $(SCN)_2$, probably forming a donor–acceptor type of complex, as already known for the molecular halogens in various aprotic solvents. Therefore the kinetic data reported above furnish the possibility of a mechanistic description of the pseudo-halogen system $(SCN)_2/SCN^-$ in acetonitrile.

The anodic *E/I* curves obtained with the rotating disk approach the shape of those corresponding to processes with a significant activation polarisation contribution, comprising the dependence of the anodic half-wave potential on the logarithm of the rotation speed.[19,20]

As the limiting current plateau of the anodic oxidation of SCN^- ion follows the predictions of the equations of the rotating disk electrode, the evaluation of the experimental diffusion coefficient, D, of the reacting species at the anode can be attempted after considering that there is one electron per SCN^- ion involved, and the kinematic viscosity of the solution at −5°C is 8×10^{-3} cm²/s. After applying Newman's equation[21] $D_{SCN^-} = 2{\cdot}14 \times 10^{-5}$ cm²/s.

The results obtained from the voltammetric runs show that both the anodic and cathodic reactions are slow electrochemical processes. At low potentials they are under activation control and at high potentials, due to the depletion of the reacting species at the electrode surface, they become diffusion-controlled. These conclusions

are derived from (i) the linear dependences of I_{ap} and I_{cp} on the square root of v (ii) the linear dependences of E_{ap} and E_{cp} on the logarithm of v and (iii) the linear $E/\log I_p$ relationship both for the anodic and cathodic maxima, involving the slope $2{\cdot}3(2RT/F)$ for the anodic as well as the cathodic reactions.

On the other hand, on the basis that the voltammetric E/I curves imply an irreversible charge-transfer mechanism, the diffusion coefficient of the species reacting on the anode can also be obtained from

$$I = nFAc_0\sqrt{(\pi Db)}\psi(bt), \tag{2}$$

where n is the number of electrons participating in the reaction per reacting particle, its bulk concentration is c_0 mole/cm^3, A is the electrode area, cm^2, b is the ratio $\alpha n_a Fv/RT$; n_a is the number of electrons involved up to the rate determining step; $\psi(bt)$ is a function of b and time t, which at the current maximum equals 0·4958.[22] Assuming that $\alpha n_a = 0{\cdot}5$, the diffusion coefficient at -4°C comes out as $2{\cdot}45 \times 10^{-5}$ cm^2/s, in good agreement with the result calculated from the rotating disk.

From the cyclic voltammetry runs it is also possible, again using (2), to estimate the diffusion coefficient of $(SCN)_2$ from the true cathodic current peak. For the purpose it is assumed that the amount of substance formed during the anodic half-cycle stays at the electrochemical interface to be completely reduced back to SCN^- ion. This implies that no side chemical reaction interferes during the voltammetric experiment. Then, the factor 0·95 relating I_{ap} to I_{cp} may be assigned to the ratio of the diffusion constants of the species reacting during the corresponding half-cycle of the voltammetric run. Thus the estimated value for $D_{(SCN)_2}$ at -4°C is $1{\cdot}98 \times 10^{-5}$ cm^2/s. The diffusion coefficients of the SCN^- ion and $(SCN)_2$ are comparable in magnitude to those already reported for the Cl^- ion and Cl_2 molecule in ACN.[15] From these results one concludes that the solvodynamic radius for the SCN^- ion is close in size to that of the Cl^- ion. This conclusion for these ions in ACN solutions agrees also with the transport behaviour they exhibit in dimethylsulphoxide, as recently reported.[23]

Possible reaction pathways related to the anodic and cathodic processes

Let us discuss the possible reaction pathways that can explain the kinetic parameters derived for both the anodic and the cathodic reactions.

Under steady state conditions the slope of the anodic Tafel line is $2RT/F$. This Tafel slope is easily deduced from one of the following reaction mechanisms,

$$\text{I} \qquad SCN^- + Pt \xrightarrow{\text{r.d.s.}} Pt(SCN) + e, \tag{Ia}$$

$$2\,Pt(SCN) \rightleftarrows (SCN)_2 + 2\,Pt; \tag{Ib}$$

$$\text{II} \qquad SCN^- + Pt \rightleftarrows Pt(SCN) + e, \tag{IIa}$$

$$Pt(SCN) + SCN^- \xrightarrow{\text{r.d.s.}} (SCN)_2 + Pt + e, \tag{IIb}$$

where Pt represents an active site at the electrode surface and (SCN) is an adsorbed radical formed during the initial electron-transfer step.

Let us assume for simplicity the symmetry factor implied in the electrode processes is 0·5, and that the intermediate follows a Langmuir adsorption isotherm. Then a Tafel slope of $2RT/F$ results immediately if reaction (Ia) is rate-determining under a

negligible degree of surface coverage by the reaction intermediate. Analogously, the same Tafel slope arises at high anode potentials from mechanism II, when step IIb, under a degree of surface coverage by reaction intermediates approaching unity.[24]

The possible mechanistic participation of the pseudotrihalide ion $(SCN)_3^-$, which would be equivalent to I_3^-, Br_3^- or Cl_3^-, has been neglected, through the argument that there are reasonable indications the equilibrium constant for trihalide formation diminishes from the I_2/I^- system to the Cl_2/Cl^- system[25,26] and that the value of the latter is small enough to prevent the existence of a trihalide oxidation and reduction E/I waves,[15] as occurs for the $SCN^-/(SCN)_2$ system.

Other possible reactions that may contribute, particularly at higher SCN^- ion concentration, are the following polymerization reactions,

$$x(SCN)_2 \rightarrow (SCN)_{2x} \qquad \text{(III)}$$

and

$$(SCN)_2 + ACN \rightarrow \text{polymer.} \qquad \text{(IV)}$$

The interference of these reactions becomes negligible at temperatures below 0°C. At higher temperatures the rate of polymerization becomes appreciable and the product formed on the electrode alters the mechanism of the reaction, as is described in other publications.[11,12]

Similarly, the cathodic reaction can be explained in terms of mechanism I or II, involving in principle the same rate-determining steps. Although no further information is yet available, due to the complexity of the system, there are various indications in favour of mechanism II as the more likely, as discussed further on. The fact that the anodic and cathodic E/I curves belong to complementary electrode reactions allows the evaluation of the apparent exchange current density, i_0, at the reversible potential of the $(SCN)_2/SCN^-$ couple. The latter should be located at a mean distance between the potentials corresponding to the anodic and cathodic current maxima in the voltammetric runs. Its value, with respect to the initial potential, is $E_0 = 0{\cdot}382 \pm 0{\cdot}005$ V. Therefore the anodic and cathodic $E/\log I$ curves deduced from voltammetric experiments can be drawn together, as shown in Fig. 11, on the new potential scale. The i_0 value calculated from Fig. 11 is $4{\cdot}46 \times 10^{-5}$ A/cm² at −3°C and $c_0 = 2{\cdot}028 \times 10^{-3}$ M. This figure is close to that obtained for the Cl_2/Cl^- electrode in ACN solution on platinum.[15]

If the i_0 value is expressed as a rate constant at equilibrium we have $k_0 = 1{\cdot}10 \times 10^{-4}$ cm/s. This rate constant can also be obtained from the variation of peak potential separation,[27] which yields $k_0 = 1{\cdot}25 \times 10^{-4}$ cm/s.

Since the SCN^- ion and $(SCN)_2$ are considered from the structural point of view as equivalent to the halide ions and halogen molecules respectively, their kinetic behaviour should be similar to that of the halogen electrodes in aprotic solvents.

The kinetics of the $I_2/I^-/I_3^-$, $Br_2/Br^-/Br_3^-$ and Cl_2/Cl^- couples in acetonitrile solutions[13–15] exhibits a degree of irreversibility of the process which increases from iodine to chlorine. The kinetic data obtained for the $(SCN)_2/SCN^-$ couple either for the convective-diffusion-controlled process as well as the activated electrode reaction is coherent with those earlier deduced for the halogen electrodes, resembling more closely that of the Cl_2/Cl^- electrode. As in that system, only one current plateau is involved in the anodic as well as the cathodic E/I curves. The apparent exchange cd is about the same as that of the Cl_2/Cl^- electrode.

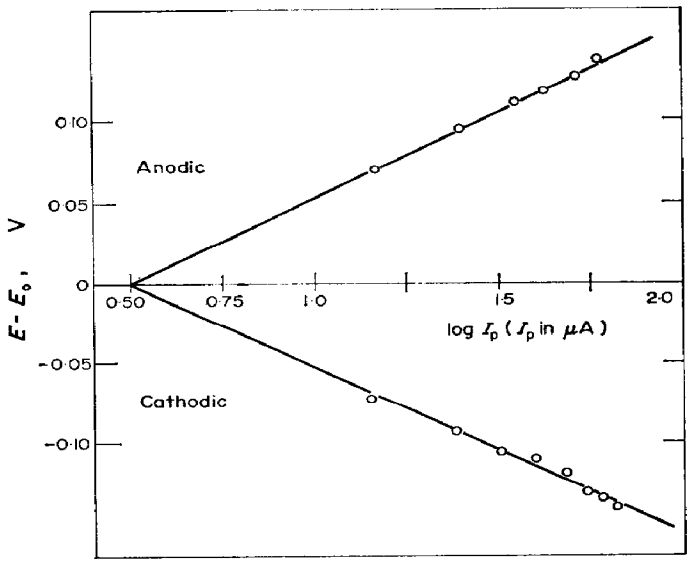

FIG. 11. Semilogarithmic plot of data shown in Fig. 7, the overpotentials being defined with respect to the apparent reversible potential of the $SCN^-/(SCN)_2$ couple.

From these considerations a preference of reaction mechanism II over reaction mechanism I seems reasonable for the $SCN^-/(SCN)_2$ system, in correspondence with the formal mechanism obeyed by the halogen electrodes in ACN.[13,15]

The mechanism implies a high degree of surface coverage by reaction intermediates. Then, the accumulation of the latter at the electrochemical interface should be the cause of the lower polarization observed at the rotating disk electrode either in the returning E/I curves or in the E/I curves recorded on platinum electrodes repeatedly used.

Acknowledgement—The research program of INIFTA is sponsored by the Universidad Nacional de La Plata, the Consejo Nacional de Investigaciones Científicas y Técnicas of Argentina and the Comisión de Investigaciones Científicas de la Provincia de Buenos Aires. R. P. participated in this work under a leave of absence from the Instituto Nacional de Tecnología Industrial (INTI) during 1970.

REFERENCES

1. H. KERSTEIN and R. HOFFMANN, *Ber.* **57**, 491 (1924).
2. R. GAUGUIN, *Annls. Chim.* **4**, 832 (1949).
3. R. GAUGUIN, *Analyt. chim. Acta* **5**, 200 (1951).
4. O. A. SONGINA and I. M. PAVLOVA, *Izv. Vysskikh. Uchebn. Zav. Khim. i Khim. Teckhnol.* **5**, 378 (1962).
5. M. M. NICHOLSON, *Analyt. Chem.* **31**, 128 (1959).
6. J. L. WOOD, in *Organic Reactions*, ed. R. ADAMS, Vol. III, p. 240. Wiley, New York (1946).
7. A. P. TOMILOV, *Russ. chem. Revs.* **30**, 639 (1961).
8. G. CAUQUIS and G. PIERRE, *C.r. Acad. Sci., Paris* **266**, 883 (1968).
9. R. PEREIRO, A. J. CALANDRA and A. J. ARVÍA, in preparation.
10. C. MARTINEZ, A. J. CALANDRA and A. J. ARVÍA, *Electrochim. Acta*, in press.
11. A. J. CALANDRA, M. E. MARTINS and A. J. ARVÍA, *Electrochim. Acta* **16**, 2057 (1971).
12. A. J. ARVÍA, A. J. CALANDRA and M. E. MARTINS, *Electrochim. Acta* **17**, 741 (1972).
13. V. A. MACAGNO, M. C. GIORDANO and A. J. ARVÍA, *Electrochim. Acta* **14**, 335 (1969).
14. T. IWASITA and M. C. GIORDANO, *Electrochim. Acta* **14**, 1045 (1969).
15. L. SERENO, V. A. MACAGNO and M. C. GIORDANO, *Electrochim. Acta* **17**, 561 (1972).
16. C. MARTINEZ, J. WARGON and A. J. ARVÍA, *Electrochim. Acta*, in press.
17. J. F. O'DONNELL, J. T. AYRES and C. K. MANN, *Analyt. Chem.* **37**, 1161 (1965).

18. R. S. NICHOLSON, *Analyt. Chem.* **38,** 1406 (1966).
19. P. DELAHAY, *New Instrumental Methods in Electrochemistry*, Chap. 6. Interscience, New York (1966).
20. G. CHARLOT, J. BADOZ-LAMBLING and B. TRÉMILLON, *Les Réactions Electrochimiques*, Chap. 2. Masson, Paris (1959).
21. A. J. ARVÍA and S. L. MARCHIANO in *Modern Aspects of Electrochemistry*, ed. J. O'M. BOCKRIS and B. E. CONWAY, Vol. 6. Plenum, New York (1971).
22. R. S. NICHOLSON and I. SHAIN, *Analyt. Chem.* **36,** 706 (1964).
23. NENG-PING YAO and D. N. BENNION, *J. electrochem. Soc.* **118,** 1097 (1971).
24. B. E. CONWAY, *Theory and Principles of Electrode Processes.* Ronald, New York (1965).
25. J. C. MARCHON, *C.r. Acad. Sci., Paris* **267,** 1123 (1968).
26. R. L. BENOIT, M. GUAY and J. DEBARRES, *Can. J. Chem.* **46,** 1261 (1968).
27. R. S. NICHOLSON, *Analyt. Chem.* **37,** 1351 (1965).